

Development of 3D Printing Technology for the Manufacture of Flexible Electric Double-Layer Capacitors

Milad Areir, Yanmeng Xu, David Harrison, John Fyson and Ruirong Zhang

Department of Design, College of Engineering and Physical Sciences, Brunel University London, Uxbridge, UB8 3PH, United Kingdom

Corresponding author: Milad Areir (milad.areir@brunel.ac.uk)

Abstract: This paper presents a novel process and manufacturing system for the fabrication of Electric Double-Layer Capacitors (EDLCs) as energy storage devices. It shows an approach for printing multilayer EDLC components using 3D printing technology. A dual nozzle deposition system was used based on a fused deposition modelling (FDM) process. This process allows layers of activated carbon (AC) slurry, gel electrolyte and composite solid filaments to be printed with high precision. This paper describes the detailed process of deposition of the AC and gel electrolyte using the dual nozzle system. It describes the energy storage performance of the printed supercapacitors in relation to differences in thickness in the AC printed layers. A supercapacitor based on printed AC and composite materials displays a specific capacitance of 38.5 mF g^{-1} when measured at a potential rate change of 20 mV s^{-1} and a current density of 0.136 A g^{-1} .

Keywords: 3D Printing technology, activated carbon, gel electrolyte, electric double-layer capacitors (EDLCs), energy storage system.

Development of 3D Printing Technology for the Manufacture of Flexible Electric Double-Layer Capacitors

1. Introduction

There is an ever-increasing need for flexible electronic devices such as flexible displays, electronic solar cells and flexible energy storage devices, especially flexible supercapacitors [1]-[7]. Supercapacitors, also known as EDLCs, are electrochemical energy storage devices that are lightweight, low cost and of high power density. EDLCs consist of three components: two electrodes with a current collector on each electrode separated by a gel electrolyte. EDLCs take advantage of the electro-ionic charge storage that can be induced in the electrochemical double layer of high-surface area carbons immersed in an electrolyte [8]. EDLCs generally show a higher power density and better cyclic stability than pseudocapacitors [9], but they have a relatively low energy density. There are many fabrication techniques used to produce active layers for supercapacitors, for instance, a light scribe DVD burner [1], spray coating [2], screen printing [3], coating [4], ink-jet printing [10], selective laser melting [11] and 3D FDM printing [12]. However, these methods require a long fabrication time and pre-treatment techniques. The challenge is to develop a simple, inexpensive fabrication method that does not require coating blades or masks as used by Zhang et al [4]. Currently, only a few attempts have been made to produce supercapacitors by 3D printing technologies [11]. Sun et al. [7] have printed graphene-based interdigitated microelectrodes for flexible planar micro-supercapacitors using a desktop XYZ motor. Zhao et al. [11] designed a 3D interdigitated electrode using a 3D selective laser-melting machine and coating method, which showed a high specific capacitance of 4.6 F cm^{-3} at a scan rate 20 mV s^{-1} . A flexible composite 3D EDLC of multilayer structure with an operating voltage of 1V with a sulfuric acid (H_2SO_4) gel electrolyte has not been reported before. This paper describes the first use of a 3D dual printing method for FDM and paste deposition to produce supercapacitors for energy storage. Open source 3D printing machines should allow a freedom of design and fabrication of 3D EDLCs with remarkably complex geometric structures.

Scott Crump registered the original FDM patent in 1992 and is co-founder of the Stratasys Company [13]. This additive fabrication process utilizes very accurate deposition to incrementally melt and deposit thin layers of flexible filaments or conductive paste to complete a 3D structure. It provides a facile and cost effective approach to producing a 3D structure. The material in this study was printed with a low-cost Reprap system, Ultimaker®, and produced a range of functional EDLCs. The FDM printing machine is limited by the types of head that can print the materials [14]. Dual printing can be used in this work. The main principle of dual printing is extruding a thin filament of molten thermoplastic by a heated nozzle onto a heated build platform as in FDM technology, while another nozzle sequentially deposits paste materials, whose flow is controlled by a Discov3ry® paste extruder as found in Fab@Home [15]. The challenge for our 3D dual printing process is to manage this technique and control where the filaments are deposited.

Development of 3D Printing Technology for the Manufacture of Flexible Electric Double-Layer Capacitors

Minimising the quantity of conductive and active material in the final printed sample is attractive. As well as the paste being printable, it needs to have the appropriate rheological properties [16]. The characteristics of conductive and activated materials will be determined by investigating the effect of solvent and particle size that is needed to achieve a printing formulation. The mass of the AC and its thickness needs to be controlled and an electrode-electrolyte interface with many different particle sizes needs to be tested. It is an advantage to measure these characteristics for many applications, in particular for an energy storage system [6]. In this work, EDLCs were designed and manufactured; the electrochemical performance of the 3D printed EDLC was investigated made with a 3D printed AC electrode using H₂SO₄ based gel electrolytes [17]. This gel electrolyte was chosen because of its low cost and non-flammability when compared to organic electrolytes. The particular novelty reported in this paper is to look at the areas of control needed to make EDLC components and with different layer thickness. This is an important factor as it affects electrolyte ions being transported between the layers of the two electrodes.

2. Experimental

2.1 Materials

Silver conductive paint with a volume resistivity of 0.001 $\Omega \cdot \text{cm}$ was purchased from RS[®] Components Ltd. Flexible LAYWOO-FLEX 3 mm diameter filament was obtained from Kai Parthy (Germany). All other materials including the AC powder, sodium carboxymethyl cellulose (CMC, MW 250,000), polyvinyl alcohol (PVA, MW 146,000~186,000, 99+% hydrolysed) and sulfuric acid (H₂SO₄, 1.80-1.84 g cm⁻³) were supplied by Sigma-Aldrich.

2.2 AC slurry electrode preparation

The active material chosen for EDLCs electrodes was reported in a previous paper by Zhang et al [4]. This AC slurry was the most challenging material to deposit. It is relatively inexpensive and of high chemical stability. The electrodes were printed using an AC, which was made into a paste with a small amount of PVA to act as a binder with a high dielectric strength in water. Higher binding strengths between the individual particles lead to considerably higher shape stability of the 3D part [18]. To provide a printable paste matrix for the EDLCs, the AC slurry was made with 2 g of PVA, which was dissolved in 40 mL distilled water to give 5% wt/vol at 50°C with 1 hour of stirring. This was mixed with 2 g of AC

Development of 3D Printing Technology for the Manufacture of Flexible Electric Double-Layer Capacitors

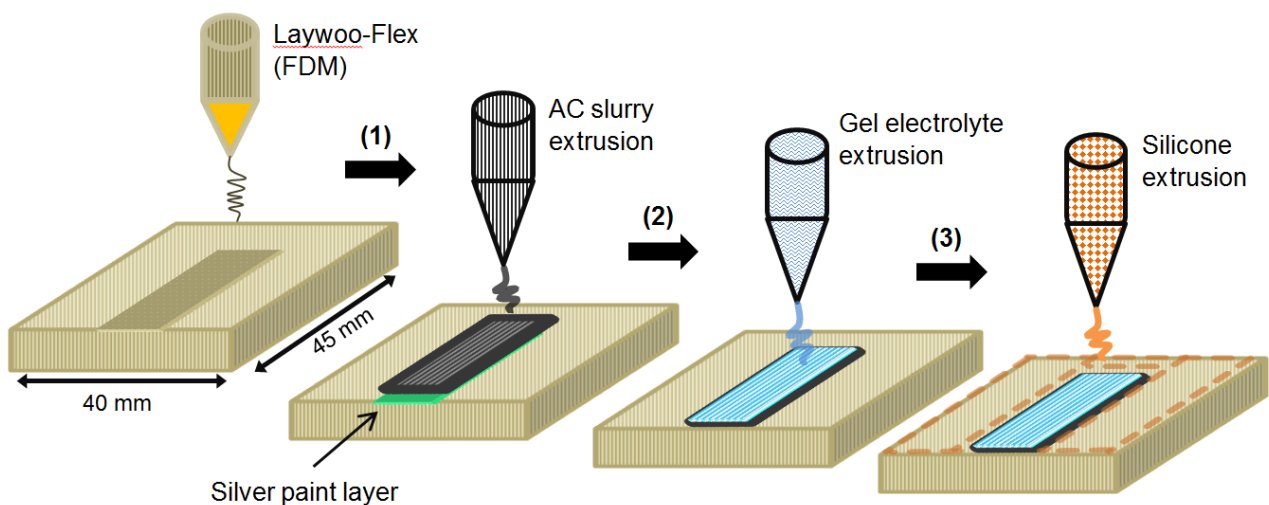
powder that had been already preheated to 100°C for 1 hour to ensure max capacity. This mixture was stirred overnight to make a homogenous slurry.

2.3 H₂SO₄/PVA gel electrolyte preparation

The gel electrolyte was prepared by dissolving 1 g of PVA powder in 20 mL of distilled water stirred at 50°C for 1 hour. An aqueous solution of H₂SO₄ was added to the aforementioned solution to obtain a final concentration of 1.6 mol dm⁻³. In order to tailor the rheology, 0.8 g of 5% wt/vol CMC binder was added. The mixture was magnetically stirred overnight. These materials were chosen for extrusion through a 0.6 mm diameter nozzle. The issues that arose during deposition were alleviated by material reformulation.

2.4 Manufacture the model supercapacitors

Deposition of patterned structures of AC slurry and printing new composites allowed the use of a wide number of different materials and processes. The main goal was to reduce manufacturing time and reduce waste material during extrusion printing and filament formation. The FDM process deposits the filament in a layer-by-layer technique. The EDLC frame parts were printed as shown in Fig. 1 step (1) using a flexible composite material LAYWOO-FLEX. Laywoo flexible composite material created with 65% copolyesters and 35% recycled wood has a comparatively lower tensile strength and a high degree of elasticity. After printing the frame parts, they were removed from the build plate and a 20 mm length of conductive copper tape was connected to the electrode bottom for electrical contact to two layers of silver paint applied with a brush which served as current collectors.



Development of 3D Printing Technology for the Manufacture of Flexible Electric Double-Layer Capacitors

Fig. 1 Schematic illustrations of EDLC fabrication.

The part was returned to the build plate for step (2) to deposit several thicknesses of AC slurry by Discov3ry[®] extrusion of a 0.6 mm layer height in a rectilinear infill pattern structure at a feed-rate of 21000 steps per mm. The extrusion used a linear stepper motor with a 100:1 planetary gear ratio pushing on a 30 cc syringe to obtain the speed that gives the right output flow rate. The AC and gel electrolyte must be viscous enough to be extruded from a syringe at room temperature yet hold its shape once extruded. The AC filaments deposited were exactly parallel on the consecutive layers. This was repeated with the same parameters for the gel electrolyte layer as shown in Fig. 1 step (3). As shown in Table 1, in order to demonstrate the prevention of any contact between the two AC electrodes, the fill density of gel electrolytes that serves as a separator and ion conductor were fixed to 100%, 60% and 30% for model A, B and C, respectively. Finally, the top surface outline perimeters were sealed by depositing a 1 mm of silicone layer that acted as a rubber gasket to ensure an excellent adhesion between the two parts of the EDLCs. The assembled EDLCs as shown in Fig. 2 were sandwiched and kept for half hour under vacuum at room temperature to give the volumetric capacitances as shown in Table 1.

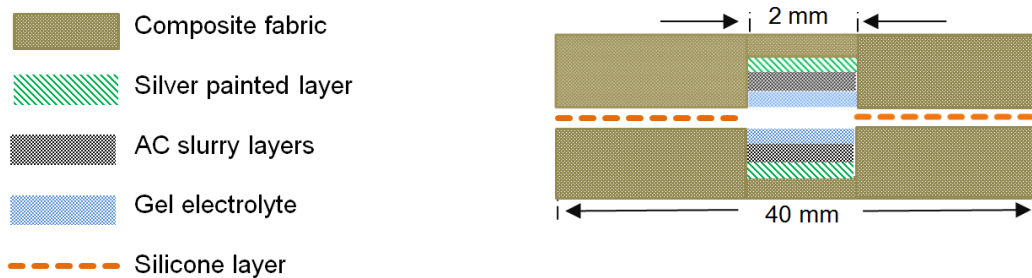


Fig. 2 Schematic structure of an EDLC.

2.5 Electrochemical measurements

Three flexible composite EDLCs of each model were assembled to test the electrochemical properties of the electrodes by using a VersaSTAT 3.0 (Princeton Applied Research) electrochemical workstation. The cyclic voltammetry (CV) tests were conducted over the potential window 1V at different scan rates 20, 50 and 100 mV s⁻¹. From the CV curve, we can calculate capacitance using the equation

$$C = \frac{Q_{\text{total}}/2}{\Delta V} \quad (1)$$

Development of 3D Printing Technology for the Manufacture of Flexible Electric Double-Layer Capacitors

Where C is the capacitance in farads (F), Q_{total} is the supercapacitor charge in coulombs (C) and ΔV is the voltage range in volts (V). Galvanostatic charge-discharge (GCD) measurements were also carried out in $1.6 \text{ mol dm}^{-3} \text{ H}_2\text{SO}_4/\text{PVA}$ electrolyte at charging current 15 mA. The capacitance can be calculated from GCD curves using

$$C = \frac{i \cdot \Delta t}{\Delta V} \quad (2)$$

Where i is the discharge current in amperes (A), Δt is the discharging time (s) and Δv is the voltage of the discharge (V). The specific capacitance (C_s) of the supercapacitor device can be calculated using

$$C_s = \frac{i \cdot \Delta t}{m \cdot \Delta V} \quad (3)$$

Where i is the current in amperes (A), Δt is the discharging time (s), m is the total mass of the active materials of the two electrodes (g) and Δv is the voltage of the discharge with exception of iR drop (V).

3. Results and discussion

Table 1 EDLCs Parameters and performance.

	Model A	Model B	Model C
Thickness (mm)	1	2	3
Layer height (mm)		0.6	
AC mass (g)	0.11	0.22	0.33
AC density, ρ (g cm^{-3})		1.375	
Fill density (%)	100	60	30

Development of 3D Printing Technology for the Manufacture of Flexible Electric Double-Layer Capacitors

H ₂ SO ₄ /PVA density, ρ (g cm ⁻³)	6.75	2.68	1.58
Current (mA)		15	
Potential window (V)		1	
Discharging time (s)	0.4	0.3	0.2
Capacitance at 20 mV s ⁻¹ (mF)	25.6	29.4	25.4
Capacitance at 50 mV s ⁻¹ (mF)	18.5	25.3	16.4
Capacitance at 100 mV s ⁻¹ (mF)	14.3	21.9	14.5
GCD capacitance (mF)	7.3	5.9	3.9
Specific Capacitance (mF g ⁻¹)	38.5	26.9	11.9

3.1 Experimental results

The results from this experiment are shown in Table 1. This summarizes the relationship between the AC and gel electrolyte laydown. It can be deduced from the Table that the thickness of each electrode had some influence on the energy storage of the samples. Many factors influence the performance of AC printed electrodes. The thickness of the electrode hinders its conductivity as the electrode mass increased and the specific capacity decreased. The type of AC including particle size, surface composition, heat treatment and the permeability of PVA binder, 3D printing fill density, infill pattern structures and filament substrate such as Laywoo-flex may be important. The particle size of the porous AC is important, as is the shape in the 3D deposition process to prevent clogging of the printing nozzles; AC has been milled for up to 72 hours at ambient temperature by ball milling to enhance the flow and reduce the internal friction when extruded. Beyond this, it could affect the capacitance behaviour due to a change in the AC particle size distribution [19]. The AC matrix-composite slurry comprises particles with an average diameter of approximately 100 nm. Fill density is an important factor in 3D printed electronics since the quantity of printed materials directly affects the cell capacity and it should be higher than 20%. For example, less than 20% of fill density of the electrode or electrolyte layer will cause holes and therefore shorts. In addition, these AC structures can affect the stability of the current collector layers and gel electrolyte. It could be the effect of the air permittivity of the frames and the airflow affects the conductive materials. This might affect the activated materials that have been tested in the capacitors after 24 hours using the electrochemical workstation and the energy storage disappears. In addition, the gel electrolyte leaks through infill structures. Therefore, the higher fill density of printed materials, the higher lifetime of the energy storage. The gel electrolyte contained corrosive strong H₂SO₄ presenting oily structures that stick well when printed onto the electrode surface. It is not advisable to use this gel with a 3D open frame

Development of 3D Printing Technology for the Manufacture of Flexible Electric Double-Layer Capacitors

machine as the acid presents a hazard and might cause serious burns to a user in comparison to a gel electrolyte based on phosphoric acid (H_3PO_4).

3.2 Flexible composite EDLC characterization

A supercapacitor has been fabricated using the prepared AC slurry which was sized to make volumes of 0.08, 0.16 and 0.24 cm^3 for model A, B and C, respectively. The cell was assembled as shown in Fig. 3 by placing the two AC electrodes parallel to each other, the gel electrolyte was between and sealed by silicone to avoid electrolyte leakage.

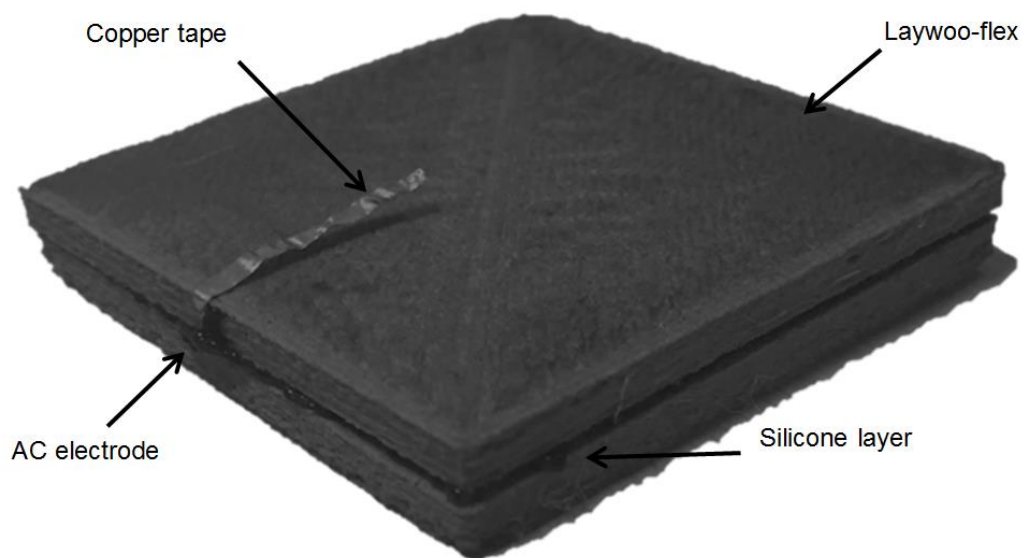


Fig. 3 Image of the flexible composite EDLC.

CV profiles of AC slurry at 20 mV s^{-1} using $\text{H}_2\text{SO}_4/\text{PVA}$ as gel electrolyte with a 1V potential window for the three supercapacitors of model A, B and C are shown in Fig. 4. The outcomes show typical shaped curves at 20 mV s^{-1} .

Development of 3D Printing Technology for the Manufacture of Flexible Electric Double-Layer Capacitors

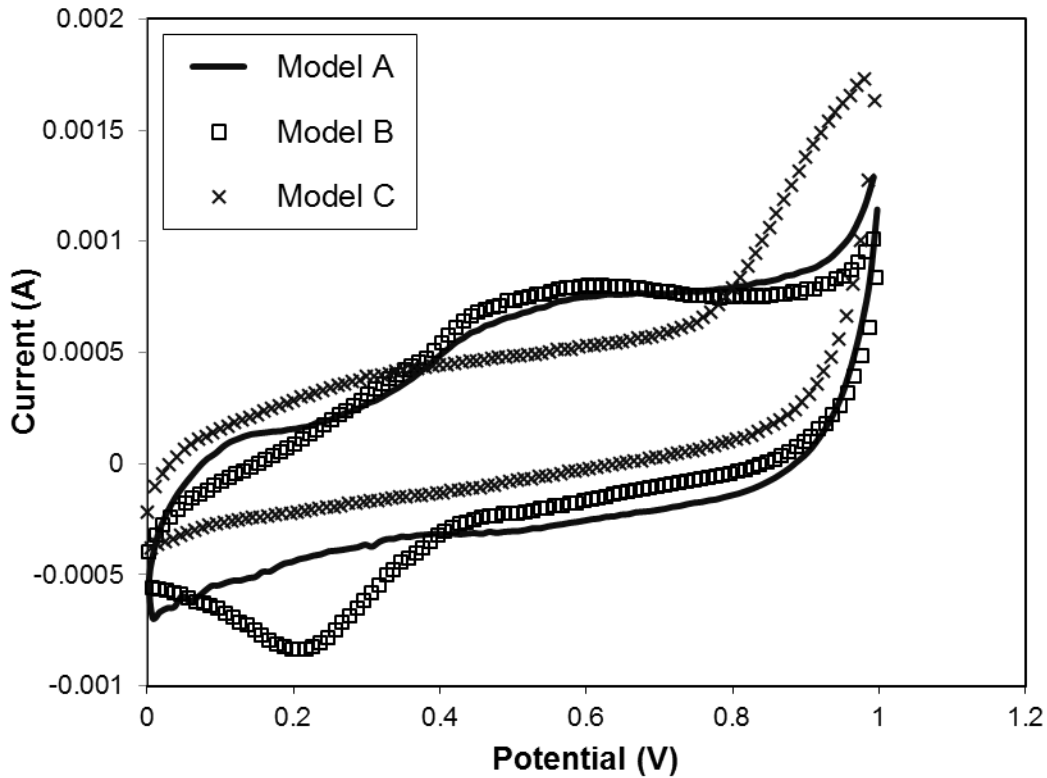


Fig. 4 CV curves obtained from the EDLCs with different AC electrodes thickness at a scan rate of 20 mV s^{-1} .

It can be seen that there is an initial oxidation on the CV curve. It might be due the current flow from electrode to electrolyte. This shows that the EDLCs performance is not the same with material of different thickness. The ability to retain an ideal rectangular shape in the 1 mm EDLC is much better than that in the 3 mm EDLC. This might be due to the series resistances of 100% fill density for gel electrolyte in 1 mm EDLC or the copper tape resistance and an electrical resistance of the porous carbon. It has been noticed that the 20 mm length conductive copper tape with 5 mm underneath the AC electrodes loses its structure and breaks within 48 hours. This could be because of the high acid density. H_2SO_4 was used in the gel electrolyte, in comparison with a gel electrolyte based on H_3PO_4 where the copper tape remains connected for a longer time. The capacitance of a supercapacitor may depend heavily on the total electrolyte-accessible surface area (EASA) of the electrodes [5]. The EDLCs capacitance is proportional to the EASA of the electrode, which is electrochemically active in storing charges. Faradaic behaviour was observed for model B and A in comparison with model C. This could be generated by the reduction in model B and by oxidation in model A. The electrode is corroding which demonstrated the instability of the silver painted layer. Faradaic reaction is competing with the capacitor surface reaction.

Development of 3D Printing Technology for the Manufacture of Flexible Electric Double-Layer Capacitors

The capacitance of the model A, B and C supercapacitors were calculated to be 25.6 mF, 29.4 mF and 25.4 mF at 20 mVs^{-1} , respectively. It has been found that these devices had a lower capacitance after 24 hours. This anomaly could be for many reasons. One reason could be that the composite material filament structure becomes easy to break if the filament is kept unsealed in an air environment for some time before printing. In this case it can be difficult to print the filament, and the feeder motor cannot push it to the hot end for extrusion. It is not recommended to print any filament material after a change in its properties during storage. The capacitance value of model A at a scan rate of 100 mV s^{-1} was 14.3 mF measured from the CV curve calculated by Eq. (1). While using GCD testing, this showed that the capacitance decreased dramatically to half, 7.3 mF, when calculated by Eq. (2). The fifth cycle GCD curves run at charging current of 15 mA for the three supercapacitors are shown in Fig. 5. If compared to capacitance calculated from the GCD curve based on the Eq. (2), it can be seen that the value of the capacitances increased with decreasing AC thickness. From the CV curves shown in Fig. 4 increasing the AC layer thickness can be seen to decrease the capacitance. Also, from Table 1 we can see that the capacitance value decreases when the thickness of the AC and $\text{H}_2\text{SO}_4/\text{PVA}$ gel electrolyte laydown increases.

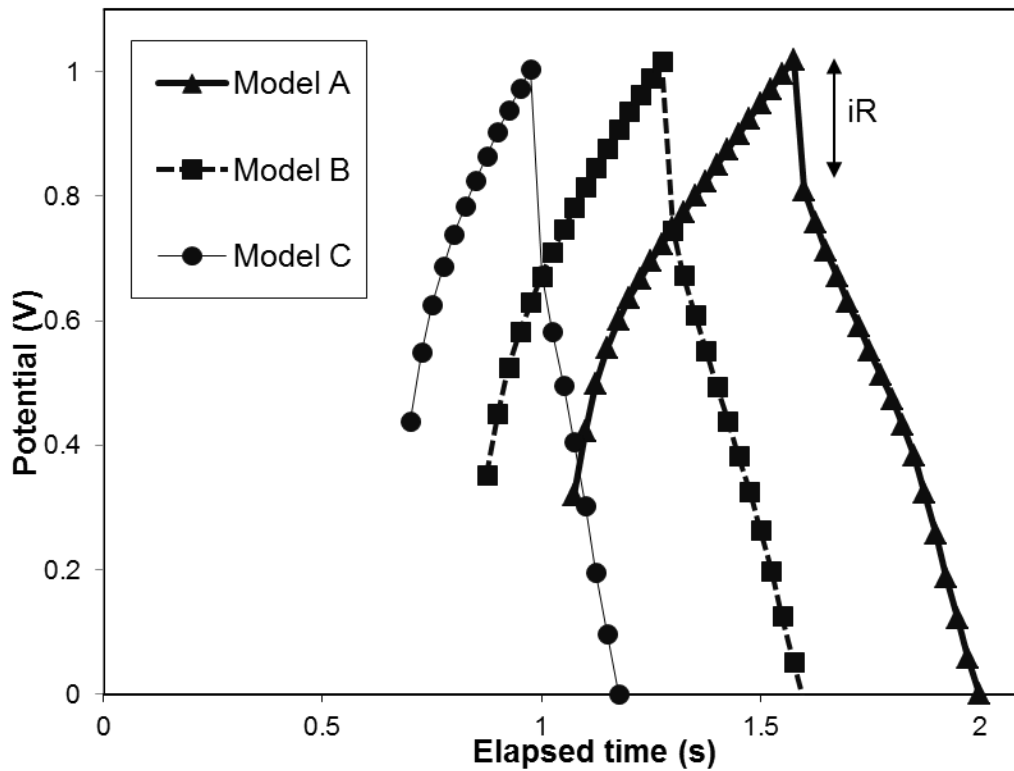


Fig. 5 GCD curves obtained from the capacitors with different AC electrodes thicknesses at a charging current of 15 mA.

Development of 3D Printing Technology for the Manufacture of Flexible Electric Double-Layer Capacitors

The iR is a voltage drop at the beginning of each discharge curve shown in Fig. 5. From Eq. (3) the assembled supercapacitor exhibited a specific capacitance of 38.5 mF g^{-1} , 26.9 mF g^{-1} and 11.9 mF g^{-1} for 1 mm, 2 mm and 3 mm thickness, respectively. A comparison of specific capacitances of composite supercapacitors with three different electrode thicknesses in $1.6 \text{ mol dm}^{-3} \text{ H}_2\text{SO}_4/\text{PVA}$ gel electrolyte is shown in Fig. 6.

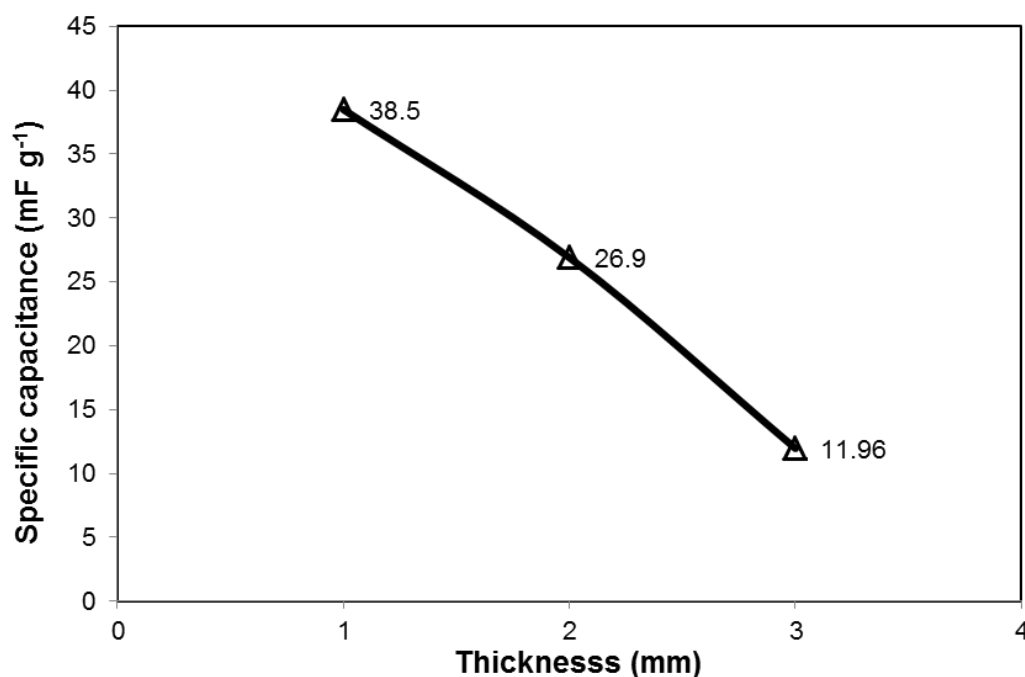


Fig. 6 C_s curve for several AC electrodes thickness.

It was expected that an increase the thickness of AC layers might lead to an increase in the specific energy stored. However, it has been noticed in our samples that as the AC thickness increased from 1 mm to 2 mm the specific capacitance decreased approximately 30% from 38.5 mF g^{-1} to 26.9 mF g^{-1} and dramatically decreased in the 3 mm capacitor to 11.9 mF g^{-1} . The electrode mass might be expected to contribute to the further energy storage as increased about 100% from 0.11 g to 0.22 g and increased a further 50% in 3 mm capacitor to reach 0.33 g. Which is mainly due to the sample sizes of the electrode. There seems to be little correlation between the mass of AC and the thickness of gel electrolyte. The increase of the specific capacitance of the composite EDLCs may increase proportionally with the decrease of the AC thickness. It could be due to the time of electrolyte diffusion processes and ions cannot move faster through the high viscosity of the 3D printed AC.

Development of 3D Printing Technology for the Manufacture of Flexible Electric Double-Layer Capacitors

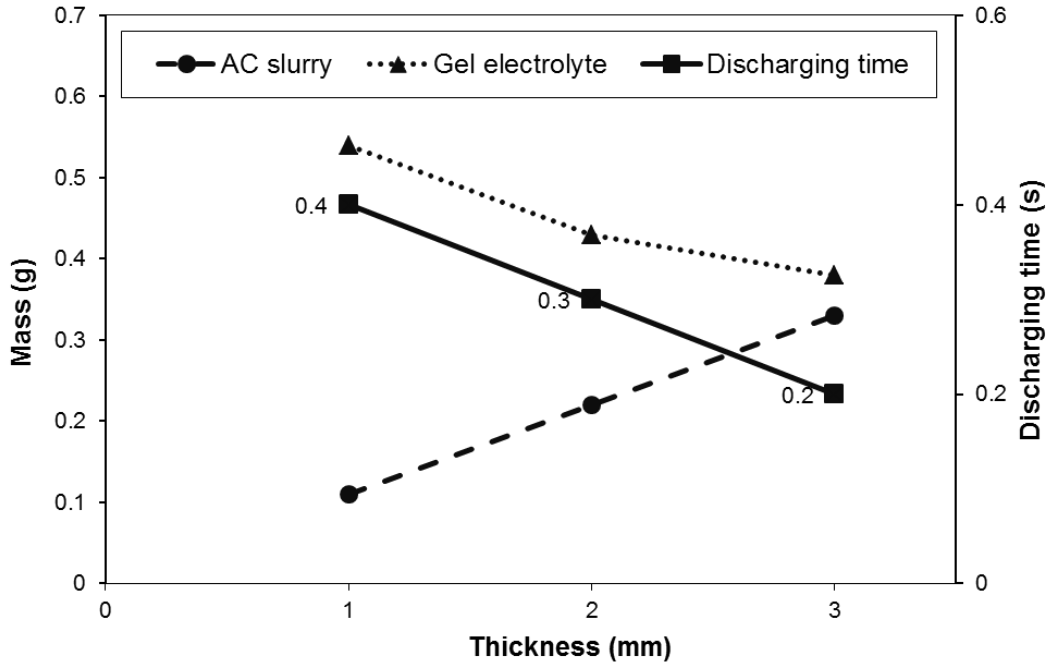


Fig. 7 The discharging time (s) vs AC and gel electrolyte (g) curve for several AC electrodes thickness (mm).

It can be seen from Fig. 7 that the discharging time slightly decreased as the AC electrodes thickness increased, (the experiment was carried out at a constant current of 15 mA and 1V). This is illustrated by the 1 mm thickness composite electrodes having an ideal EDLCs behaviour with a short charge/discharge period of less than 0.4 s. In addition, it had long lifetime storage at 0.3 mF in comparison with the GCD curves of model B and C, which were overlapping. Gel electrolyte ion concentration may play a role in separating the two electrodes. As shown in Table 1, with an optimum density 2.68 g cm^{-3} laydown percentage of $\text{H}_2\text{SO}_4/\text{PVA}$ gel electrolyte with 2 mm thickness of AC slurry, the capacity value was higher measured by a CV curve. With an approximate 73% increase of gel electrolyte laydown, the AC slurry discharging time was 0.3 s. Sa'adu et al. have enhanced the quality of the polymer electrolyte and reduced the thickness of the electrode to increase the capacitance [20]. The energy density and power density are calculated based from the GCD curves by the Eq. (4) and (5).

$$E = \frac{1}{2} C_s V^2 \quad (4)$$

$$P = \frac{E}{\Delta t} \quad (5)$$

Development of 3D Printing Technology for the Manufacture of Flexible Electric Double-Layer Capacitors

Where E is energy density, C_s is the specific capacitance, v is the potential window, Δt is the discharging time and P the power density. The highest energy density of the AC supercapacitor is obtained in model A reaching 0.019 Wh kg^{-1} with a corresponding power density of 165.0 W kg^{-1} with $1.6 \text{ mol dm}^{-3} \text{ H}_2\text{SO}_4/\text{PVA}$ gel electrolyte. While in model B and C have energy densities of 0.013 Wh kg^{-1} and 0.006 Wh kg^{-1} with a corresponding power densities of 124.1 W kg^{-1} and 55.4 W kg^{-1} , respectively. Thus, AC based EDLCs generally has the disadvantage of lower energy density when operated with gel electrolytes compared to organic electrolytes [21], [22]. High dielectric constants are used to increase an energy density for EDLCs.

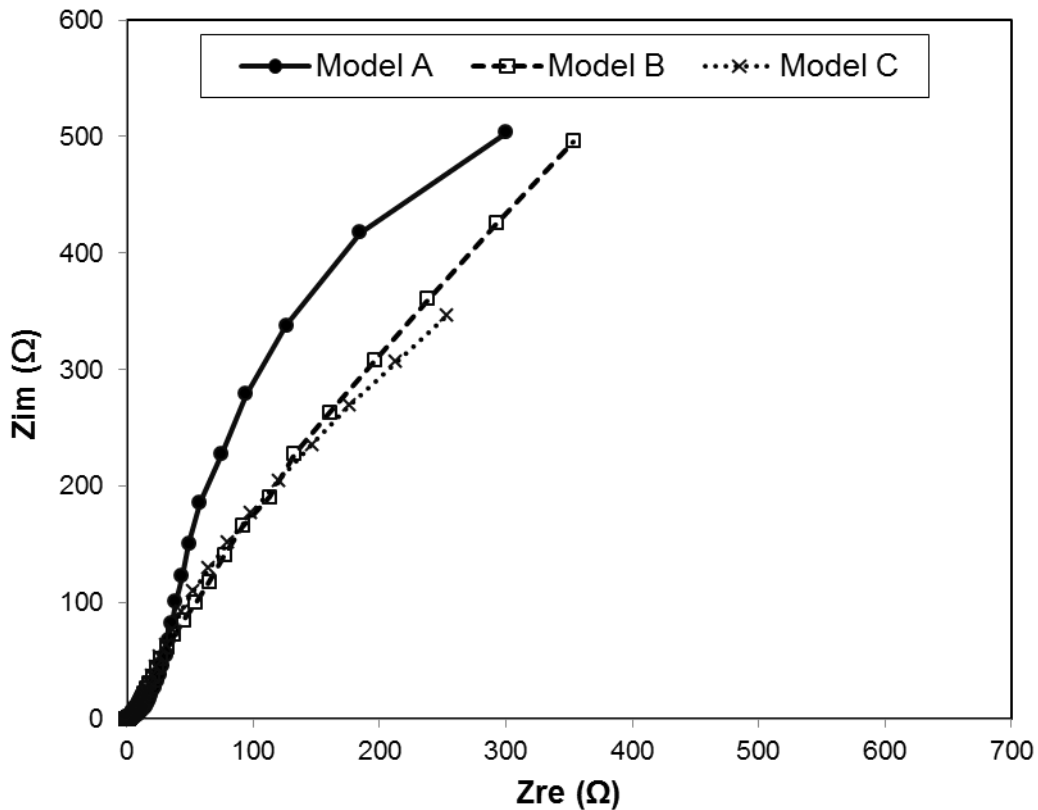


Fig. 8 Nyquist plot performed at 0 V with frequency range from 100 kHz to 0.01 Hz.

As shown in Figure 8, the smaller equivalent series resistance (ESR) might lead a larger power density [22]. An ESR difference can be explained in terms of the conductivity of gel electrolyte. Using the electrochemical impedance spectroscopy (EIS) technique with a frequency range of 0.01 Hz-100 kHz.

$$\text{ESR} = \frac{V_{iR}}{i} \quad (6)$$

Where V_{iR} is the iR drop at charge and discharge (V) and i is current in amperes (A). The iR drop of model A in the GCD curve for $1.6 \text{ mol dm}^{-3} \text{ H}_2\text{SO}_4/\text{PVA}$ electrolyte was approximately 0.13 V due to its

Development of 3D Printing Technology for the Manufacture of Flexible Electric Double-Layer Capacitors

100% fill density. While model B and C the iR were about 0.23 V. Slight similar values of the iR for potassium nitrate (KNO_3) and H_3PO_4/PVA electrolytes have been reported [23]. ESR were measured at the start frequency 100 kHz going to 0.01 Hz and were calculated by Eq. (6) and are 8.6 Ω , 13.3 Ω and 15.3 Ω for model A, B and C, respectively. It can be seen from Fig. 8 that ESR curves for model B & C are quite similar but different from model A which has a different slope. It is valuable to see that the semicircle nearly vanishes in the Nyquist plot for model B and C. It might be due to the value of a different contact resistance, leading to less hindering of ion transfer and in addition, high frequency could lead the current leakage. Water separation from H_2SO_4/PVA gel electrolyte during 3D deposition process played a dominant role in ESR value. The layer height was 0.6 mm and that may increase ESR in comparison with other processes. A sufficient time to let electrodes dry could help AC layers adhere well onto the current collectors, which decreases the ESR. Also extra amounts of binder content will increase the electrode resistance [24]. But 5% wt/vol PVA binder content was found to help the flow deposition with a 0.6 mm diameter tapered nozzle.

4. Conclusions

The formulated materials have enabled the rapid production of a range of EDLCs using low-cost 3D printing. The results revealed several interesting features of the FDM and paste deposition processes. Highly versatile and cost effective material processing techniques demonstrate substantial technical advantages compared with other fabrication techniques due to the potential for making different, multiple material forms. The 3D flexible composite EDLCs were successfully manufactured and characterized in this work. The AC slurry and gel electrolyte were printed successfully in a rectilinear infill pattern. This approach resulted in a relatively low printing time of less than 2 minutes for each AC and gel electrolyte fill structures. The AC slurry used has exceptional electrochemical performance. It has been shown that the process is a promising technique to manufacture complex and accurately shaped structures. This might allow a greater freedom in the design of supercapacitors produced by dual nozzle deposition systems. The EDLCs can still be optimized for further improved resolution by controlling the tool paths and infill patterns. This is an important area for further research including choosing an infill pattern for the active material and gel electrolyte.

References

Development of 3D Printing Technology for the Manufacture of Flexible Electric Double-Layer Capacitors

- [1] M.F. El-Kady, R.B. Kaner, Scalable fabrication of high-power graphene micro-supercapacitors for flexible and on-chip energy storage, *Nature communications*, 4 (2013) 1475.
- [2] H.T. Jeong, B.C. Kim, M.J. Higgins, G.G. Wallace, Highly stretchable reduced graphene oxide (rGO)/single-walled carbon nanotubes (SWNTs) electrodes for energy storage devices, *Electrochimica Acta*, 163 (2015) 149-160.
- [3] S.M. Yoon, J.S. Go, J. Yu, D.W. Kim, Y. Jang, S. Lee, J. Jo, Fabrication and Characterization of Flexible Thin Film Super-Capacitor with Silver Nano Paste Current Collector, *Journal of nanoscience and nanotechnology*, 13(12) (2013) 7844-7849.
- [4] R. Zhang, Y. Xu, D. Harrison, J. Fyson, F. Qiu, D. Southee, Flexible strip supercapacitors for future energy storage, *International Journal of Automation and Computing*, 12(1) (2015) 43-49.
- [5] Q. Zhou, X. Ye, Z. Wan, C. Jia, A three-dimensional flexible supercapacitor with enhanced performance based on lightweight, conductive graphene-cotton fabric electrode, *Journal of Power Sources*, 296 (2015) 186-196.
- [6] F. Qiu, D. Harrison, J. Fyson, D. Southee, Fabrication and characterisation of flexible coaxial thin thread supercapacitors, *Smart Science*, 2(3) (2014) 107-115.
- [7] G. Sun, J. An, C.K. Chua, H. Pang, J. Zhang, P. Chen, Layer-by-layer printing of laminated graphene-based interdigitated microelectrodes for flexible planar micro-supercapacitors, *Electrochemistry Communications*, 51 (2015) 33-36.
- [8] D. Dubal, O. Ayyad, V.P. Gómez-Romero, Hybrid energy storage: the merging of battery and supercapacitor chemistries, *Chemical Society Reviews*, 44 (7) (2015) 1777-1790.
- [9] S. He, L. Chen, C. Xie, H. Hu, S. Chen, M. Hanif, H. Hou, Supercapacitors based on 3D network of activated carbon nanowhiskers wrapped-on graphitized electro spun nanofibers, *Journal of Power Sources*, 243 (2013) 880-886.
- [10] H. Pang, Y. Zhang, W. Lai, Z. Hu, W. Huang, Lamellar $K_2Co_3(P_2O_7)_2 \cdot 2H_2O$ nanocrystal whiskers: High-performance flexible all-solid-state asymmetric micro-supercapacitors via inkjet printing, *Nano Energy*, 15 (2015) 303-312.
- [11] C. Zhao, C. Wang, R. Gorkin, S. Beirne, K. Shu, G.G. Wallace, Three dimensional (3D) printed electrodes for interdigitated supercapacitors, *Electrochemistry Communications*, 41 (2014) 20-23.
- [12] J.H. Kim, W.S. Chang, D. Kim, J.R. Yang, J.T. Han, G. Lee, J.T. Kim, S.K. Seol, 3D printing of reduced graphene oxide nanowires, *Advanced Materials*, 27(1) (2015) 157-161.
- [13] I. Gibson, D. Rosen, B. Stucker, Additive manufacturing technologies: 3D printing, Rapid prototyping and direct digital manufacturing, Springer, (2014).

Development of 3D Printing Technology for the Manufacture of Flexible Electric Double-Layer Capacitors

- [14] R. Anitha, S. Arunachalam, P. Radhakrishnan, Critical parameters influencing the quality of prototypes in fused deposition modelling, *Journal of Materials Processing Technology*, 118 (1) (2001) 385-388.
- [15] E. Malone, H. Lipson, Fab@Home: the personal desktop fabricator kit, *Rapid Prototyping Journal*, 13(4) (2007) 245-255.
- [16] B. Utela, D. Storti, R. Anderson, M. Ganter, A review of process development steps for new material systems in three dimensional printing (3DP), *Journal of Manufacturing Processes*, 10 (2) (2008) 96-104.
- [17] C. Zhao, W. Zheng, A review for aqueous electrochemical supercapacitors, *Frontiers in Energy Research*, Vol. 3 No. 00023 (2015).
- [18] J. Shen, Material system for use in three dimensional printing, United States: U.S. Patent and Trademark Office, DaimlerChrysler AG. 7,049,363; 2006 (2015).
- [19] N. Welham, V. Berbenni, P. Chapman, Increased chemisorption onto activated carbon after ball-milling, *Carbon*, 40 (13) (2002) 2307-2315.
- [20] L. Sa'adu, M. Hashim, M.B. Baharuddin, A Noble Conductivity Studies and Characterizations of PVA-Orthophosphoric-Filter Paper Electrolytes, *Journal of Materials Science Research*, 3 (4) (2014) 1.
- [21] Y. Chen, X. Zhang, H. Zhang, X. Sun, D. Zhang, Y. Ma, High-performance supercapacitors based on a graphene-activated carbon composite prepared by chemical activation, *RSC Advances*, 2 (20) (2012) 7747-7753.
- [22] S. Zhang, Y. Li, N. Pan, Graphene based supercapacitor fabricated by vacuum filtration deposition, *Journal of Power Sources*, 206 (2012) 476-482.
- [23] J. Bae, M.K. Park, Y.J. Kim, J.M. Liu, Z.L. Wang, Fiber Supercapacitors Made of Nanowire-Fiber Hybrid Structures for Wearable/Flexible Energy Storage, *Angewandte Chemie International Edition*, 50 (7) (2011) 1683-1687.
- [24] R. Zhang, Y. Xu, D. Harrison, J. Fyson, D. Southee, Experimental Design to Optimise Electrical Performance of Strip Supercapacitors, *Int.J.Electrochem.Sci*, 11 (2016) 675-684.